



33 feed more than 200 million people (Zhang, 2014). However, geohazards, such as  
34 cracking–sliding, toppling, falling, sliding, peeling, and failures of cavity built by human, occur  
35 frequently because of fragile geological and natural environments, excessive reclamation, and  
36 unreasonable engineering activities. Among these geohazards, cracking–sliding failure, normally  
37 with a volume of several hundred cubic meters, causes the largest number of casualties in the  
38 eastern LPC (Lei, 2001). More than 1000 cracking–sliding failures were recorded in the past two  
39 decades, and they caused an average of more than 100 fatalities per year despite the small  
40 volumes of individual failures. Unlike “flows” or “slides” as defined by Cruden and Varnes  
41 (1996), cracking–sliding failures have composite failure planes composed of two parts. The  
42 upper part normally develops vertically from the crown of the slope down for one to several  
43 meters deep. The upper part forms by tensile cracking, but the slope can stand stably for a long  
44 time with such cracks. The lower part is generally inclined at an angle ranging from 15° to 60°.  
45 Sliding along the lower part, which is triggered by rainfall, freezing–thawing, daily temperature  
46 fluctuations, slope undercutting, and earth tremors likely mobilizes cracking–sliding failures.

47 According to historical records, 62 cracking–sliding failures occurred in Shenmu, Mizhi,  
48 Zizhou, and other sites in Northern Shaanxi Province from 1985 to 1993 and caused 258 deaths  
49 and more than 40 injuries (Qu et al., 2001). In 2005, the cracking–sliding failure in Jixian County  
50 in Shanxi Province resulted in 24 deaths and economic losses of approximately RMB 10 million.  
51 Failure with a volume of  $2.5 \times 10^4 \text{ m}^3$  took place in Zhongyang County in Shanxi on November  
52 16, 2009, causing 23 deaths and destroying 6 houses. In 2013, 36 loess failures were documented  
53 in Tianshui City, Gansu Province (Xin et al., 2013). In 2015, a cracking–sliding failure in  
54 Linxian County, Shanxi buried four families comprising nine people. All of these failures  
55 developed within the loess–paleosol sequence, with relatively uniform mineralogical and  
56 chemical compositions. More recently, a cracking–sliding failure occurred in Shilou County of  
57 Shanxi Province on March 10, 2018, and destroyed 36 houses (Fig. 1). The original loess slope  
58 was characterized by slope gradient of 60°, height of 50 m and aspect of 280°. The scarp of this  
59 failure was dominated by near-vertical tensile cracks with average gradient of 85°. The displaced  
60 mass reached 7600 m<sup>3</sup>.

61 Frequent and disastrous events demand an in-depth understanding of causative factors and  
62 development patterns of loess failures to reduce the occurrence of such geohazards. This study  
63 collects a large set of data on loess cracking–sliding failures, climate, and soil temperature to  
64 facilitate a detailed analysis of the internal and external causes of such failures. This study also  
65 emphasizes the influences of slope features (i.e., slope type, gradient, height, and aspect), rainfall,  
66 freezing–thawing cycles, daily temperature fluctuations, and human engineering activities.

## 67 **2 Study area**

68 The study area is limited to the eastern LPC and covers Northern Shaanxi and Western  
69 Shanxi provinces, considering the homogeneous background of climatic, morphologic, geologic,  
70 and anthropic conditions in these regions (Fig. 2). Elevation of the study area ranges from 800 to  
71 1300 m above sea level from southeast to northwest. The study area has a typical semiarid  
72 continental monsoon climate with four distinct seasons. The average annual rainfall in this area  
73 varies from 400 to 700 mm. Rainfall in summer (from July to September) accounts for  
74 approximately 70% of the year (Hui, 2010; Qian, 2011; Zhu 2014). For instance, the maximum  
75 precipitation in an hour in Yan'an City can accumulate to more than 60 mm in summer (Zhu,  
76 2014). The total rainfall in Shilou County reached 412 mm in a month from early July to early  
77 August in 2013 (Lv, 2011) and corresponded to 81% of rainfall in the same year. According to  
78 records for the past 10 years, the average annual temperature is relatively constant, ranging from  
79 8 °C to 12 °C. However, variations in temperature in a day can occasionally be higher than 25 °C,  
80 the highest temperature being recorded at noon and the lowest temperature at midnight.

81 The study area is located in the east of the Ordos basin. The Fenwei Graben, spanning  
82 northeast to southwest, is a tectonic depression encountering a number of normal and strike-slip  
83 faults and covering more than 20,000 km<sup>2</sup> (Huang et al., 2008; Liu et al., 2013). The thickly  
84 bedded Pleistocene loess-paleosol sequence constitutes more than 70% of the study area and  
85 reaches a maximum thickness of 300 m. From top to bottom, the loess-paleosol sequence  
86 includes Late Pleistocene Malan Loess (Q<sub>3</sub>), Middle Pleistocene Lishi Loess (Q<sub>2</sub>), and Early  
87 Pleistocene Wucheng Loess (Q<sub>1</sub>). The Malan Loess, with thickness ranging from 10 m to 30 m,  
88 is the most widespread. The Lishi Loess, with several to tens interlayers of loess and paleosol,  
89 underlies the Malan Loess and forms a 60–150 m thick layer. The Wucheng Loess is  
90 sporadically exposed along some loess gullies. Remarkable landforms, such as loess platforms,  
91 ridges, and hillocks, have been formed in the study area because of intensive surficial erosion  
92 (Zhang, 1983, 1986). Loess platforms are mainly distributed in the Luochuan area in Northern  
93 Shaanxi Province; loess ridges are mainly found in the peripheries of the Luochuan platform and  
94 the eastern regions of the Yellow River; and loess hillocks are mainly located in Yan'an, Suide  
95 and in both sides of the Yellow River between Shaanxi and Shanxi provinces.

### 96 **3 Dataset**

97 A large set of data of loess cracking-sliding failure events were collected from published  
98 literature and unpublished reports by local governments. Slope profile, gradient, height and  
99 aspect, were derived in polygon from the initiation areas. The initiation areas rather than the  
100 whole landslides were compared in the following statistical analysis. The polygons were  
101 obtained by means of 1) interpretation of remote sensing images which were taken prior to the  
102 event; 2) engineering documentation if the host slope was engineered; or 3) post-event field  
103 survey and consultation with the local population. The field survey was normally conducted  
104 within 1–2 days immediately after the event. A total of 1176 cracking-sliding events were

105 recorded in the past 20 years across the study area. Of these events, 321 were published in the  
106 literature, 670 were presented in government reports, and 185 were unpublished. All of the 1176  
107 failures were individually reviewed by verifying the reliability, accuracy, and completeness of  
108 the original records. Finally, 458 cases (red dots in Fig. 2) were selected to set up the dataset for  
109 this study by considering the completeness of the records of any type.

110 Data pertaining to rainfall were obtained from the records of 75 meteorological stations (blue  
111 dots in Fig. 2), which are almost uniformly distributed across the study area. Statistical analysis  
112 shows that the variation in average annual rainfall in the past 15 years among these stations is  
113 less than 80 mm, indicating a relatively homogeneous climatic condition over the study area.

## 114 **4 Results and discussion**

### 115 **4.1 Internal factors**

116 Loess slopes are divided into four types in terms of slope profile: rectilinear, convex, concave,  
117 and stepped slopes (Table 1). Concave and stepped slopes are more stable than the rectilinear and  
118 convex slopes. We surveyed 212 loess slopes in Lishi City in Shanxi Province and found that  
119 stepped slopes, convex slopes, rectilinear slopes, and concave slopes account for 38%, 31%, 18%,  
120 and 13% of all slopes, respectively (Fig. 3a). This finding is consistent with the conclusion of  
121 Qin et al. (2015), who performed a field survey on loess slopes in Yan'an City, Shaanxi Province.  
122 However, approximately one-half of cracking–sliding failures occur in rectilinear slopes. In Fig.  
123 3b, the statistical analysis of the 458 failure cases indicates that rectilinear slopes are the most  
124 susceptible to cracking–sliding failure (48%), followed by convex slopes (28%). Stepped (13%)  
125 and concave (11%) slopes are the least susceptible to such failures.

126 In general, the overall gradients of rectilinear and convex slopes are steep, resulting in large  
127 internal stresses and stress concentrations, particularly at the shoulder and toe sections (Table 1).  
128 The bottom part of the concave slope has a gentle gradient and has a supporting function to the  
129 steep upper part, thereby relieving the stress concentration; the maximum shear stress at the foot  
130 of concave slopes is typically only one-half of the shear stress at the foot of rectilinear slopes  
131 (Zhang et al., 2009). The stress distribution pattern in each step section of a stepped slope is  
132 similar to that of a rectilinear slope. However, the magnitude of internal stress of stepped slopes  
133 is lower than that of rectilinear slopes because of the small height of each step and the gentle  
134 overall gradient. These findings explain that most cracking–sliding failures occur in rectilinear  
135 slopes, although these slopes are not the dominant slope type in the loess area.

136 In addition to slope profile, the gradient, height, and aspect of loess slopes are closely related  
137 to the occurrence of cracking–sliding failures. Figure 4a shows that failure occurs mostly on  
138 slopes with gradients greater than  $60^\circ$  and that the number of failures increases with gradients.  
139 Of the cracking–sliding failures, 16%, 25%, and 47% occur on slopes with gradients ranging  
140 from  $61^\circ$  to  $70^\circ$ , from  $71^\circ$  to  $80^\circ$ , and from  $81^\circ$  to  $90^\circ$ , respectively. Figure 5 shows the tension

141 zones that developed at slope shoulders, where radial and tangential stresses transform into  
142 tensile stresses. The steeper the slope is, the wider the tension band is (Stacey, 1970; Zhang et al.,  
143 2009).

144 Figure 4b illustrates that slope height is another main factor controlling the occurrence of  
145 cracking–sliding failures. In the study area, most cracking–sliding failures occur on slopes with  
146 heights of 5 m to 40 m and thus account for 87% of the total number of occurrences. The  
147 remaining 13% take place on slopes with heights of more than 40 m. A high slope normally  
148 develops a gentle gradient because of long-term weathering and erosion. By contrast, a low slope  
149 generally forms a steep gradient (Zhu et al., 2011), thereby becoming prone to collapses.

150 Slopes mostly exposed to sunlight are more prone to the development of cracking–sliding  
151 failures than shady slopes (Fig. 4c). Statistical analysis shows that 69% of the cracking–sliding  
152 failures occur on slopes with aspects in the range of 90° to 270°, particularly within 180° to 270°  
153 because sunward slopes receive long sunshine hours and soil temperature is relatively high  
154 during the day. Therefore, high differences in temperature exist between day and night. Sunward  
155 slopes are generally subjected to more weathering than shady slopes, resulting in fractured  
156 structures, which are unfavorable to slope stability. Furthermore, people usually reside on  
157 sunward slopes, and dense human engineering activities exert a large degree of disturbance on  
158 the slope body, thereby increasing the occurrence of failures.

## 159 **4.2 External factors**

### 160 **1) Rainfall**

161 Rainfall remarkably influences the stability of loess slopes. In Figure 6, the number of loess  
162 failures is closely and positively correlated with the average monthly rainfall of the past 15 years.  
163 Summer rainfall (July to September) in the study area accounts for approximately 60% of the  
164 annual precipitation, and the number of cracking–sliding failures in the same period corresponds  
165 to 62% of the total failures. This finding is consistent with that of Gao et al. (2012), who  
166 indicated that more than 60% of loess failures happen in Gansu Province in the rainy season.  
167 Wei (1995) and Liu et al. (2012) presented a similar conclusion in Shanxi and Shaanxi provinces,  
168 respectively.

169 Rainfall induces loess cracking–sliding failures in three ways, namely, splash erosion, shovel  
170 runoff, and seepage. At the beginning of rainfall, soil particles with poor adhesion are separated  
171 and broken under the impact of raindrops. When potholes formed by splash erosion are filled  
172 with water, a layer of water flow forms and triggers small soil particles to move. Along with the  
173 continued rain, this water flow converges into the slope runoff to erode and destroy the slope  
174 surface further (Tang et al., 2015). In cases of persistent rainfall, preferential seepage pipes

175 usually develop inside a slope, thereby saturating the soils, reducing the shear strength, and  
176 eventually causing cracking–sliding failures.

## 177 **2) Freezing and thawing**

178 Figure 6 shows that cracking–sliding failures occur frequently not only in the rainy season  
179 from July to September but also in the winter-to-spring transition from March to April. Soil  
180 temperature increases rapidly from values below 0°C to values above 0°C. As shown in Figure 7,  
181 soil temperature remains negative, and the frozen depth can reach approximately 1.0 m  
182 underground from late November to February in the loess areas in China. At the end of March,  
183 the ground temperature begins to increase, and the frozen layer gradually enters the thawing  
184 stage. By mid-April, the soil is rapidly heated up to approximately 8 °C.

185 Freezing and thawing mainly promote the occurrence of cracking–sliding failures via two  
186 mechanisms: 1) Frost heaving damages the soil structure and reduces soil shear strength. The  
187 loess itself contains a considerable number of large pores. Frost heaving further increases the  
188 distance between soil particles, reduces the dry density of soil, and loosens the structure, thereby  
189 reducing its cohesion and internal friction angle. 2) Thawing causes the loess structure to  
190 collapse and reduce its shear strength. Thawed water can dissolve cement, especially calcareous  
191 cement, between loess particles, consequently damaging the loess structure and increasing pore  
192 water pressure; as a result, the shear strength of the soil decreases (Pang, 1986).

## 193 **3) Daily temperature fluctuation**

194 Consistent with previous findings (Wei, 1995), our results indicate a relatively high  
195 frequency of occurrence of cracking–sliding failures between 10 pm and 4 am (Fig. 8). The  
196 difference in temperature between day and night in the loess area is more obvious than that in  
197 other regions at the same latitude in China (Sun and Zhang, 2011), and variations in air  
198 temperature in a day can occasionally reach 30 °C. The soil at a 50 cm depth shows an average  
199 daily temperature difference of approximately 5 °C in summer (Fig. 9). Thermal expansion and  
200 shrinkage occur during the rapid change in day and night temperatures. Under the cyclic  
201 functioning of shrinkage and expansion stresses, a soil structure loosens.

## 202 **4) Human activity**

203 Loess areas in China have a population of more than 200 million. Human engineering  
204 activities frequently occur and mainly involve cutting slopes for buildings, excavation for cave  
205 dwellings, and construction of terraced fields and roads (Del Prete and Parise, 2013). Cutting  
206 slopes for buildings causes the side slope to become steep. Unloading-induced tensile fractures  
207 are usually produced on the trailing edge of slopes during the rapid adjustment of a stress field  
208 within a slope (Fig. 10a). When a cave is excavated, roof damage (normally caving) happens  
209 because of a local tensile stress concentration if the design of a geometric section of a cave is

210 inappropriate (Fig. 10b). Terraced fields change the original path of surface runoff and enhance  
211 rainfall infiltration. Together with irrigation, terraced fields increase the water content of loess  
212 slopes and increase their phreatic level (Fig. 10c). The majority of traffic lines in the loess area  
213 stretch along valleys and bank slopes. Slope cutting and excavation during road construction  
214 result in a large number of high and steep side slopes, which provide a suitable environment for  
215 failures (Fig. 10d).

216 More than half of the failures are attributed to human engineering activities (Fig. 11). In 2014,  
217 9 of 16 failure cases that occurred in Yan'an City were caused by extremely steep slopes for cave  
218 dwelling construction, and the 7 other cases were consequences of improper treatment of side  
219 slopes for road construction (Lei, 2001). These findings demonstrate that intense human  
220 activities likely result in a high probability of loess failures.

## 221 **5 Conclusions**

222 This study investigates the influencing factors and development patterns of loess cracking–  
223 sliding failures in the eastern LPC according to a large collection of field investigation data. The  
224 following conclusions are obtained.

225 (1) The influencing factors of cracking–sliding failures are divided into internal and  
226 external causes. Internal causes include various features, such as slope geometry, height, gradient,  
227 and aspect of loess slopes, whereas external causes comprise rainfall, freezing–thawing cycles,  
228 temperature fluctuation, and human engineering activities.

229 (2) Cracking–sliding failure more likely occurs in rectilinear and convex slopes than in  
230 concave and stepped slopes. Rectilinear and convex slope gradients are generally steep, stress  
231 concentrations are obvious, and slope stability is poor. The stress concentration in concave and  
232 stepped slopes is minimized, and stability is fair. Cracking–sliding failure more likely takes place  
233 on slopes with gradients greater than  $60^\circ$ , and the greater the gradient is, the higher the likelihood  
234 of failures. Cracking–sliding failure also tends to occur on slopes with heights of 5 to 40 m.  
235 Slopes below 5 m have low internal stress and high stability. Slopes above 40 m are generally  
236 gentle with low stress concentration. The dominant aspect of the development of cracking–  
237 sliding failure is within  $180^\circ$  to  $270^\circ$  (sunward slopes) because of the evident temperature  
238 difference between day and night and the strong weathering.

239 (3) The occurrence of cracking–sliding failure displays a particular time pattern. Within a  
240 year, its occurrence coincides with seasonal rainfall. Failures mainly occur in the rainy season, or  
241 from July to September. In addition, failures frequently take place from March to April because  
242 of freezing and thawing. Within a day, failures happen mostly from 10 pm to 4 am because of the  
243 large temperature variation between day and night.

244 (4) The more intense the engineering activities are, the greater the possibility of loess  
245 failures is. Human engineering activities in loess areas include cutting slopes for buildings,  
246 excavation of cave dwellings, and construction of terraced fields and roads. These engineering  
247 activities usually lead to a rapid change in the features and stress field of slopes. Such high and  
248 steep side slopes tend to develop unloading-induced tensile fractures, thereby increasing the  
249 possibility of loess failures.

250 *Acknowledgments.* This study was supported by the Key Program of National Natural Science  
251 Foundation of China (No. 41630640), the Major Program of the National Natural Science  
252 Foundation of China (No. 41790445), the 2014 Fund Program for the Scientific Activities of  
253 Selected Returned Overseas Professionals in Shanxi Province, Shanxi Scholarship Council of  
254 China, Outstanding Innovative Teams of Higher Learning Institutions of Shanxi, Soft-science  
255 Fund Project of Science and Technology in Shanxi, Research Project for Young Sanjin  
256 Scholarship of Shanxi, Collaborative Innovation Center for Geohazard Process and Prevention at  
257 Taiyuan Univ. of Tech., Recruitment Program for Young Professionals of China.

## 258 **References**

- 259 Cruden, D. M., and Varnes, D. J.: Landslide types and processes, In: Landslides: investigation  
260 and mitigation, Transportation Research Board Special Report., 247, 1996.
- 261 Del, Prete, S., Parise, M.: An overview of the geological and morphological constraints in the  
262 excavation of artificial cavities, In: Filippi, M., Bosak, P. (Editors), Proceedings 16th  
263 International Congress of Speleology, Brno, 21-28 July 2013, vol. 2, p. 236-241.
- 264 Gao, H., Zhang, Y. J., and Zhang, X. G.: Factors on geological hazards of loess slope in Lanzhou  
265 city, Gansu Geol., 3, 30-36, 2012.
- 266 Huang, Z., Xu, M., Wang, L., Mi, N., Yu, D., and Li, H.: Shear wave splitting in the southern  
267 margin of the Ordos Block north China, Geophys. Res. Lett., 35, 402-411, 2008.
- 268 Hui, X., Research on relationship between geo-hazard and rainfall in Loess Plateau of Northern  
269 Shanxi Province, Ph.D. thesis, Chang'an University, Xi'an, China, 2010.
- 270 Lei, X. Y.: Geohazards of Loess Plateau and their relation with human activities, Geol. Press.,  
271 2001.
- 272 Liu, J., Zhang, P., Lease, R.O., Zheng, D., Wan, J., Wang, W., and Zhang, H.: Eocene onset and  
273 late Miocene acceleration of Cenozoic intracontinental extension in the North Qinling range-  
274 Weihe graben: Insights from apatite fission track thermochronology, Tectonophysics, 584,  
275 281-296, 2012.
- 276 Liu, J. N., Gu, Y., Jin, J., Ni, S. H., and Shen, Y.: Analysis of rainfall, floods and droughts in  
277 middle Shanxi in recent years, China, J. China. Hydrol., 2, 51-54, 2013.



278 Lv, M.: The present situation of the loess collapse of geological disasters in Shanxi Province and  
279 the water sensitivity analysis, Ph.D. thesis, Taiyuan University of Technology, Taiyuan,  
280 China, 2011.

281 Pang, G. L.: A discussion on maximum seasonal frost depth of ground, China, *J. Glaciol.*  
282 *Geocryol*, 3, 253-254, 1986.

283 Pye, K.: *Aeolian dust and dust deposits*. Academic Press, London, 1987.

284 Qian, P.: Study of types for highway drainage system in loess areas in northern Shaanxi Province,  
285 Ph.D. thesis, Chang'an University, Xi'an, China, 2011.

286 Qin, L. L., Qi, Q., and Ju, Y. W.: Study on the feature governance research of loess geological  
287 disasters in Shanxi Province, China, *Shanxi Archit.*, 6, 58-59, 2015.

288 Qu, Y. X., Zhang, Y. S., and Chen, Q. L.: Preliminary study on loess slumping in the area  
289 between northern Shaanxi and western Shanxi – taking the pipeline for transporting gas from  
290 west to east in China, China, *J. Eng. Geol.*, 9, 233-240, 2001.

291 Richthofen, F.von.: On the mode of origin of the Loess. *Geol. Mag.* 9, 293-305, 1882.

292 Smalley, I., Marković, S. B., and Svirčev, Z.: Loess is [almost totally formed by] the  
293 accumulation of dust, *Quaternary International*, 240, 4-11, 2011.

294 Stacey, T. R.: The stress surrounding open-pit mine slope, In: *Planning Open Pit Mine*, 1970.

295 Sun, Z. X., and Zhang, Q.: Analysis of climate characteristics of land surface temperature and  
296 energy in the semi-arid region in the Loess Plateau, China, *J. desert Res*, 5, 1302-1308, 2011.

297 Tang, Y. M., Feng, W., and Li, Z. G.: A review of the study of loess slump, China, *Adv. Earth*  
298 *Sci.*, 1, 26-36, 2015.

299 Wei, Q. K.: Collapse hazards and its distribution features of time and space in Shaanxi Province,  
300 China, *J. Catastrophol.*, 10, 55-59, 1995.

301 Xin, C. L., Yang, G. L., Zhao, Z. P., Sun, X. H., Ma, W. Y., and Li, H. R.: Characteristics,  
302 causes and controlling of loess collapses in Beishan mountain of Tianshui city, China, *Bull.*  
303 *Soil Water Conserv.*, 33, 120-123, 2013.

304 Yang, W. Z., and Shao, M. A.: *Researches of soil moisture in Loess Plateau*, Sci. Press., 1995.

305 Zhang, Z.H.: The compilation principle of landscape type map of Chinese Loess Plateau, China,  
306 *Hydrogeology and Engineering Geology*, 2, 29-33, 1983.

307 Zhang, Z.H.: Institute of hydrogeology and engineering geology of Chinese Academy of  
308 Geological Sciences, China, *Landscape type Map and Instructions of Chinese Loess Plateau*  
309 (1:500000), Beijing, Geological Press., 1986.

310 Zhang, Z. Y., Wang S. T., Wang L. S., Huang R. Q., Xu Q., and Tao L. J.: *Engineering*  
311 *geological analysis principle*, Geol. Press., 2009.

312 Zhang, H.: Study of water migration and strength of the loess under freezing-thawing action,  
313 Ph.D. thesis, Xi'an University of Architecture and Technology, Xi'an, China, 2014.

- 314 Zhu, J. H.: Study on the relationship between slope geometrical morphology and landslide  
315 collapse disasters in Yan'an, Ph.D. thesis, Chang'an University, Xi'an, China, 2014
- 316 Zhu, Y. C., Li, J., and Ren, Z. Y.: Change tendency and relevant analysis about cultivated land  
317 and population in Loess Plateau during about 300 years, China, J. Shaanxi Norm. University  
318 (Natur. Sci. Ed.), 3, 84-89, 2011.

## Captions of figures and tables

**Table 1.** Classification of loess slopes.

**Figure 1.** The cracking-sliding failure occurred in Shilou County of Shanxi Province on March 10, 2018 (110°50'48.54"E, 36°59'54.76"N).

**Figure 2.** Geological map of the study area. The red dots denote the cracking–sliding failure cases, and the blue dots indicate the meteorological stations in the study area.

**Figure 3.** Statistical analysis results: a) classification of loess slopes in Lishi City, Shanxi Province, China, on the basis of a field survey of 212 loess slopes, indicating that stepped slopes are dominant in the study area. b) Percentage of cracking–sliding failures that occurred in different types of loess slopes across the study area, showing that rectilinear slopes are highly susceptible to loess failures.

**Figure 4.** Effect of slope features on cracking–sliding failures.

**Figure 5.** Development of tension zones in slopes of different gradients (Stacey, 1970; Zhang et al., 2009).

**Figure 6.** Occurrence of cracking–sliding failures mainly in July to September and consistent with the average monthly rainfall.

**Figure 7.** Annual variation of temperature (°C) within a shallow zone of a typical loess slope (Yang and Shao, 1995).

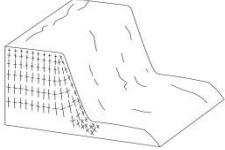
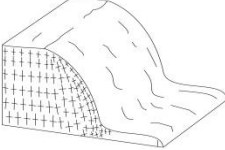

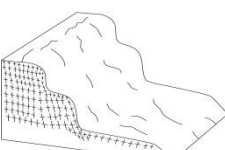
**Figure 8.** Temporal distribution of cracking–sliding failures in a day between 10 pm and 4 am.

**Figure 9.** Daily soil temperature variation in loess areas of China in summer. Data are from the field monitoring during April 2014 to September 2017 in Linxian County, Shanxi, China.

**Figure 10.** Typical engineering activities in loess areas in China: a) cut slopes for buildings; b) excavations for cave dwellings; c) terraced fields for farming; and d) cut slopes for highways.

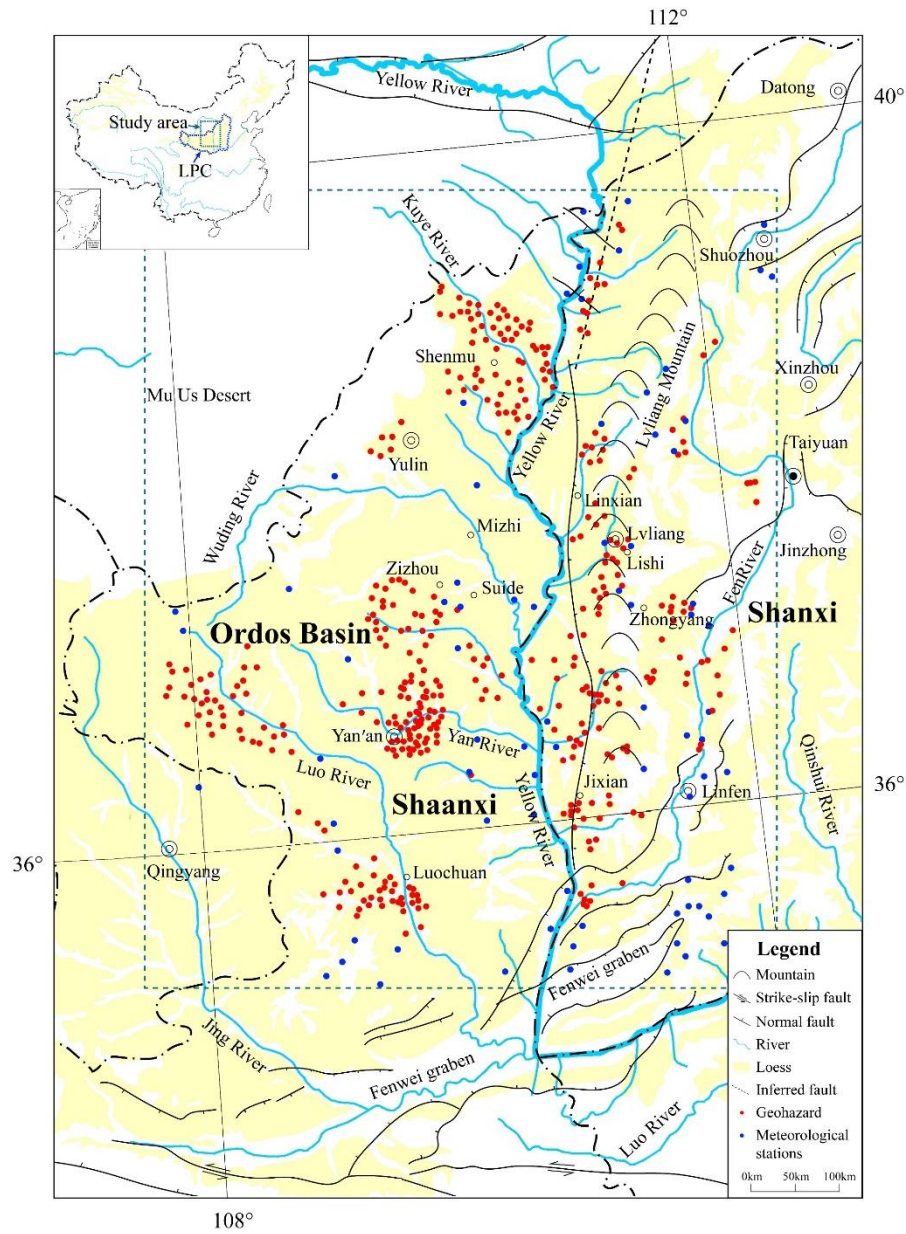
**Figure 11.** Role of engineering activities in loess failures: a) Shanxi Province; and b) Huangling County, Shaanxi Province.

**Table 1.** Classification of loess slopes.

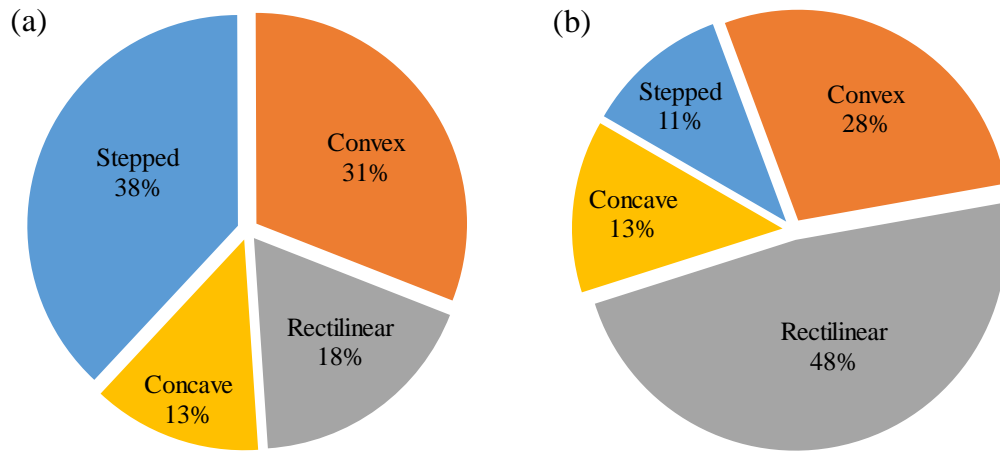
Slope type	Profile	Characteristics	Susceptibility to cracking–sliding failure
Rectilinear		Slope is straight or nearly straight; slope gradients are fairly large ( $>55^\circ$ ); stability is low.	Yes
Convex		Gentle at the top and steep at the bottom; convex shoulder; stability is generally poor.	Yes
Concave		Curves inward; gentle toward the toe supporting steep upper slope; more stable than other slopes; stability is fair.	No
Stepped		Stepped with straight faces; average gradient of the overall slope is generally small; stability is good.	No



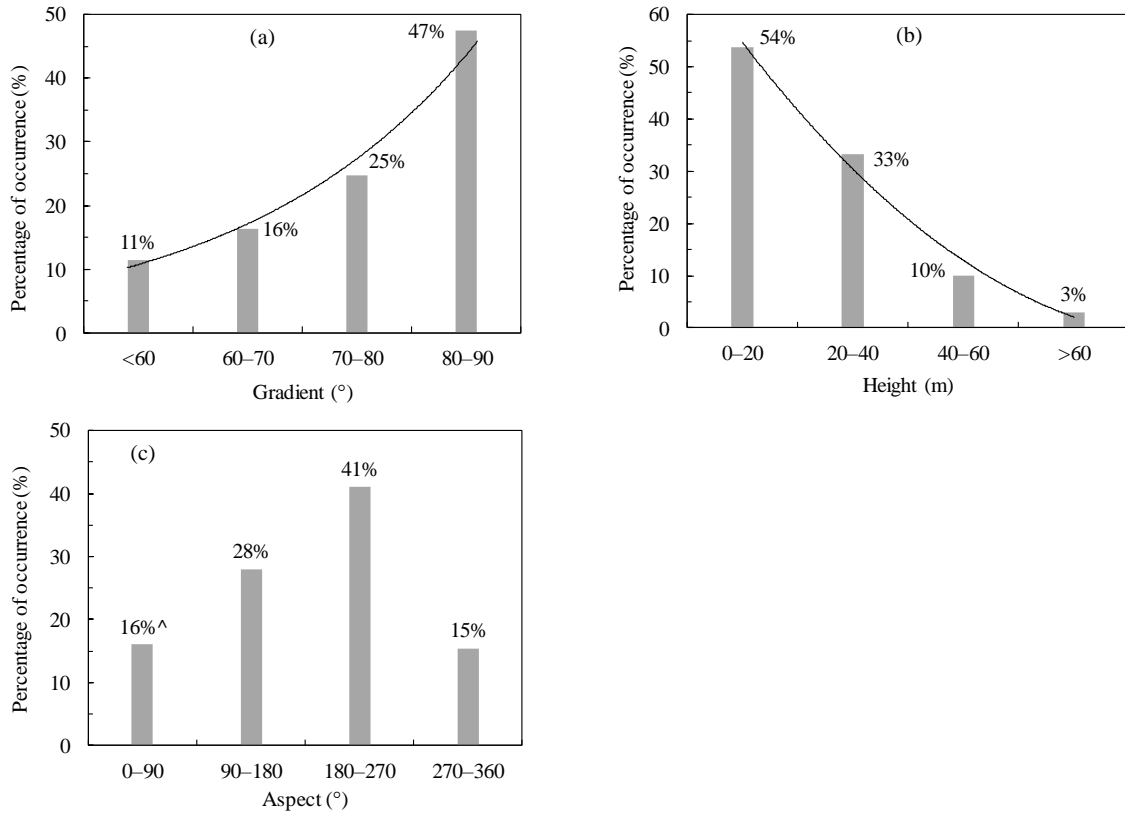
**Figure 1.** The cracking-sliding failure occurred in Shilou County of Shanxi Province on March 10, 2018 ( $110^{\circ}50'48.54''\text{E}$ ,  $36^{\circ}59'54.76''\text{N}$ ).



**Figure 2.** Geological map of the study area. The red dots denote the cracking–sliding failure cases, and the blue dots indicate the meteorological stations in the study area.

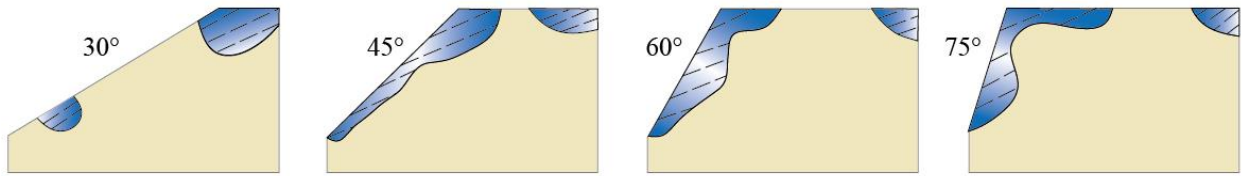


**Figure 3.** Statistical analysis results: a) classification of loess slopes in Lishi City, Shanxi Province, China, on the basis of a field survey of 212 loess slopes, indicating that stepped slopes are dominant in the study area. b) Percentage of cracking-sliding failures that occurred in different types of loess slopes across the study area, showing that rectilinear slopes are highly susceptible to loess failures.

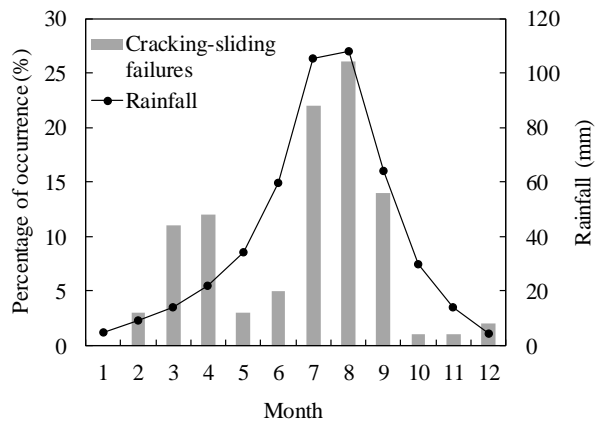


**Figure 4.** Effect of slope features on cracking-sliding failures.

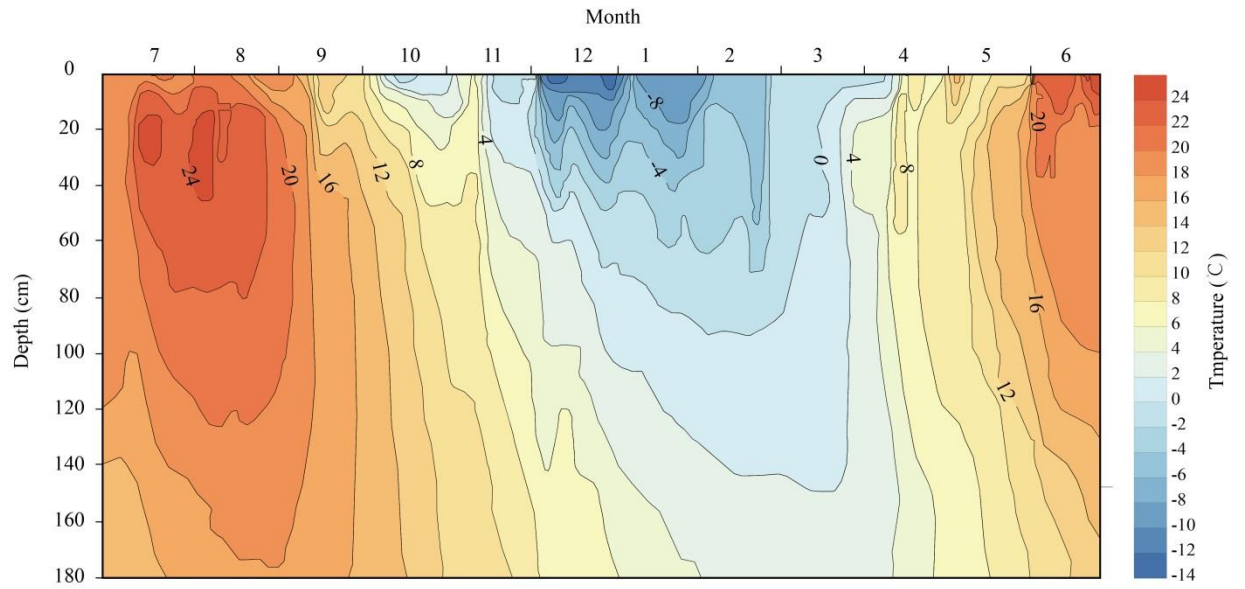




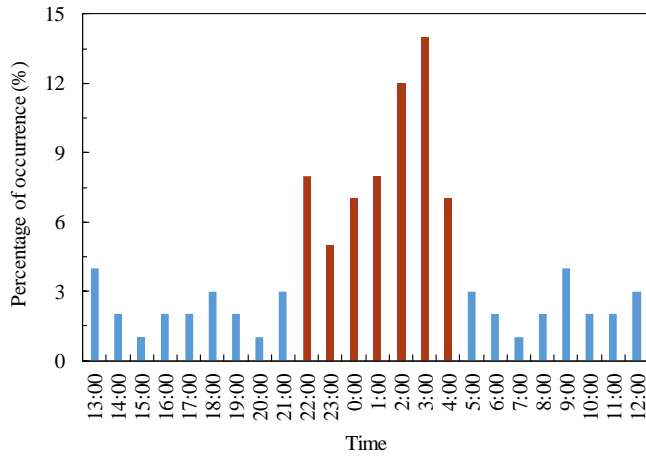
**Figure 5.** Development of tension zones in slopes of different gradients (Stacey, 1970; Zhang et al., 2009).



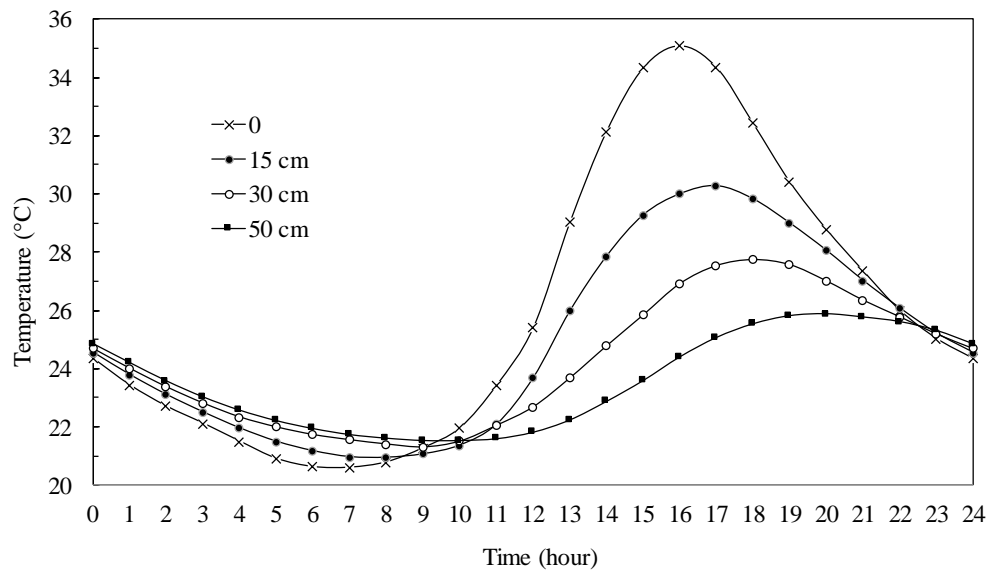
**Figure 6.** Occurrence of cracking–sliding failures mainly in July to September and consistent with the average monthly rainfall.



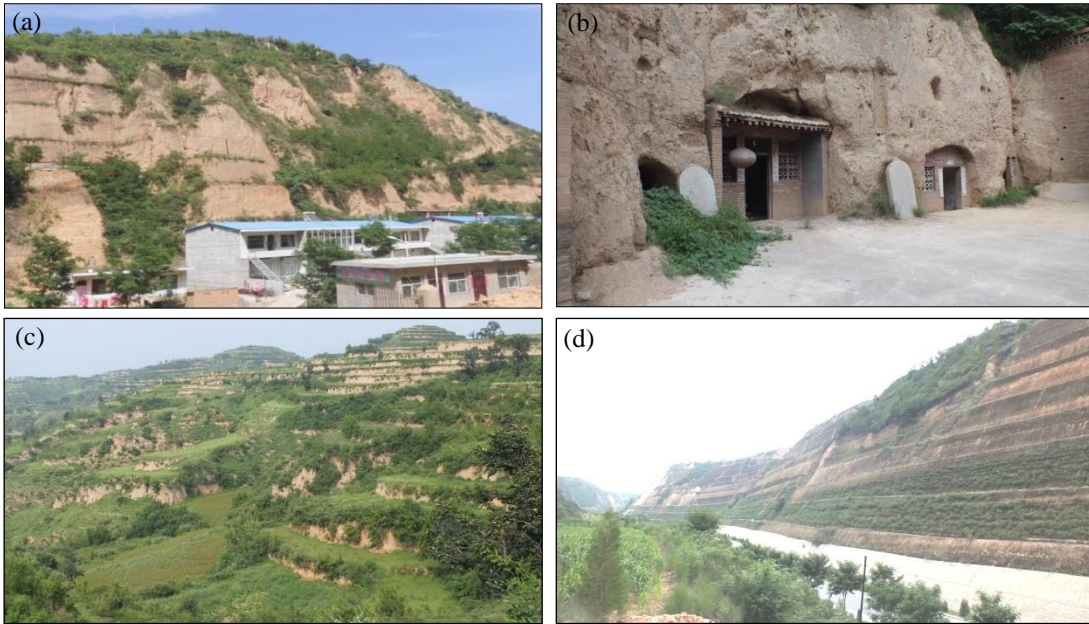
**Figure 7.** Annual variation of temperature (°C) within a shallow zone of a typical loess slope (Yang and Shao, 1995).



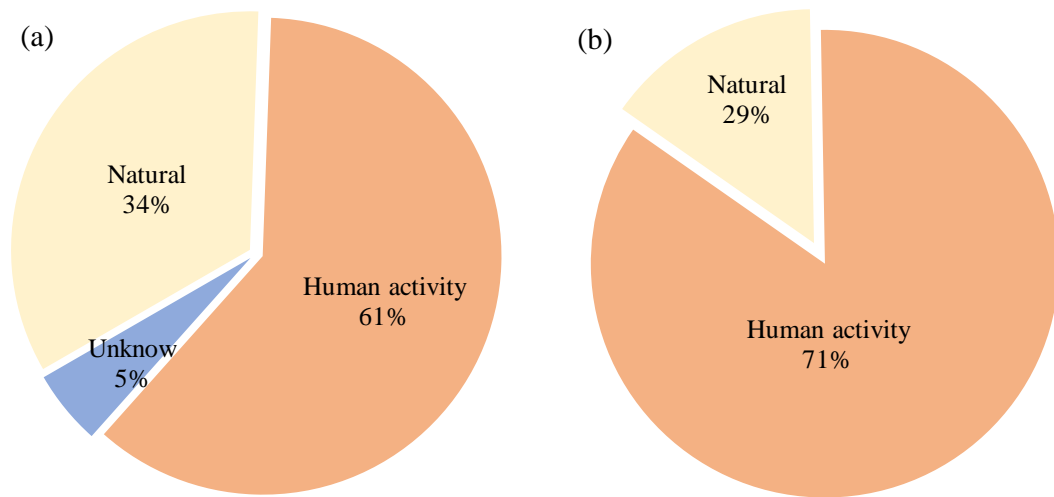
**Figure 8.** Temporal distribution of cracking–sliding failures in a day between 10 pm and 4 am.



**Figure 9.** Daily soil temperature variation in loess areas of China in summer. Data are from the field monitoring during April 2014 to September 2017 in Linxian County, Shanxi, China.



**Figure 10.** Typical engineering activities in loess areas in China: a) cut slopes for buildings; b) excavations for cave dwellings; c) terraced fields for farming; and d) cut slopes for highways.



**Figure 11.** Role of engineering activities in loess failures: a) Shanxi Province; and b) Huangling County, Shaanxi Province.